

การแก้มการ บาวดารีเลเยอร์ 2 มิติ ด้วยรูปแบบ Time-Marching โดยไม่มีการใช้ กฎความคล้ายคลึงกัน

วันชัย อัครภูษิตกุล¹
มหาวิทยาลัยเทคโนโลยีพระจอมเกล้าธนบุรี

สำนักห้องสมุดและบรรณสารสนเทศ
มหาวิทยาลัยเทคโนโลยีพระจอมเกล้าธนบุรี

บทคัดย่อ

การวิเคราะห์ชั้นบาวดารีเลเยอร์ ที่เกิดขึ้นจากการไหลของของไหลบนพื้นผิวของวัตถุ มีความสำคัญอย่างมากในการทำนายพฤติกรรมการไหลของของไหล บทความนี้เสนอเทคนิคการแก้มการบาวดารีเลเยอร์ 2 มิติ ที่สามารถประยุกต์กับพื้นผิวที่ซับซ้อนได้ โดยเขียนรูปสมการให้อยู่ในแกนที่สัมผัสและตั้งฉากกับพื้นผิวของวัตถุที่วิเคราะห์ จากนั้นเปลี่ยนรูปสมการการคำนวณที่ได้ อยู่ในกริดที่คงที่ ด้วยวิธี body-fitted curvilinear โดยไม่มีการใช้กฎความคล้ายคลึงกัน (similarity law) คำตอบของตัวแปรที่เกี่ยวข้องกับเวลาจะวนหาคำตอบจนได้คำตอบที่สภาวะเสถียร เทคนิคการแก้มการนี้ได้ผ่านการทดสอบ และยืนยันผลที่ได้เทียบกับ ข้อมูลจากการทดลอง

¹ อาจารย์ ภาควิชาวิศวกรรมเครื่องกล

SOLUTION OF NON-SIMILAR 2D BOUNDARY LAYERS USING A TIME-MARCHING SCHEME

Wanchai Asvapoositkul ¹

King Mongkut's University of Technology Thonburi

Abstract

A method is presented for the solution of 2D boundary layer equations by using a time-like algorithm in which the time-dependent boundary-layer equations are marched in time until the steady solution is found. The governing equations are numerically solved without employing the similarity law and transformed into a body-fitted curvilinear computational domain. Therefore, the computation is general and can be applied to flow over complex models. The method is applied to a number of experimental test cases, where excellent agreement between predictions and measurements is obtained.

¹Lecturer, Department of Mechanical Engineering

INTRODUCTION

In the current survey, there are a number of studies which have been done to develop a technique to capture viscous flows by using Navier-Stokes equations. In most of these methods, the flow near the wall is not resolved due to computational restriction on the grid size and therefore an empirical wall function is used to model the effect of viscous layer at the wall. The wall function can be roughly thought of as a solution to the boundary-layer momentum equation using Prandtl's mixing-length turbulence model when convective and pressure gradient terms are insignificant. However, there is no strong evidence of similarity profile particularly for 3D boundary layers. Therefore, the wall function limits the ability of Navier-Stokes methods to accurately predict the flow. One way to obtain a better resolution at the wall with little computational cost is to use a so-called zonal approach. In a zonal approach, the boundary layer equations are solved at the solid boundary in a fine grid and the Navier-Stokes equations are solved outside the boundary layer in a coarse grid together with appropriate matching boundary conditions. The Navier-Stokes solutions provide an outer boundary condition for 'boundary equations in the viscous layer. In return, the boundary layer solutions provide information near the solid boundary. The solutions are advanced simultaneously on a coarse and on a fine grid. Methods outlined for zonal formations may be seen in Tang and Hafez [1] and Hafez et al. [2].

This paper outlines the first phase of a project for the development of one such zonal method for turbomachinery calculations. This phase of the work is mainly concerned with the development of an efficient boundary layer solver which its implementation and application are simple and straightforward.

The methods for solving boundary-layer equation have a common technique that the partial differential equations of the boundary layer are transformed to one having an algebraic representation [3]. The methods differ only in the implementation of the marching schemes. A summary of many methods was prepared by Cebeci and Smith [4], and White [5]. Simple methods and numerical considerations related to the finite difference solution of the boundary layer equations were described in two excellent books by Anderson et al. [3] and Fletcher [6].

Lakshminarayana [7] reviewed and assessed various computational fluid dynamic techniques for the analysis and design of turbomachinery. He recommended that the boundary-layer equations for turbomachinery flow should be written in a curvilinear system and a rotating cylindrical co-ordinate. These would enable the equations to account for the effects of rotation and surface curvature. These set of equations was derived by Yamazaki [8] and was applied to calculate the boundary-layer on propeller blades by Groves and Change [9] and Oshima [10].

A fully implicit finite difference approximation of the boundary layer equations was developed by Zangeneh and Asvapoositkul [11]. The method was based on space-marching scheme and was constrained by stability and zone of dependence conditions. Another approach is based upon a time-like algorithm in which the constraints were relaxed [12].

GOVERNING EQUATIONS

Since boundary layer equations are defined on curved surface of the body, the equations should be transformed to the curvilinear system $(\bar{\xi}, \bar{\zeta})$. A straightforward procedure is to use the metric stretching h to relate the curvilinear co-ordinate to a standard co-ordinate system (e.g. Cartesian co-ordinate) [8]. In this co-ordinate, $\bar{\xi}$ is defined along the body surface and $\bar{\zeta}$ is the actual distance measured normal to $\bar{\xi}$. The relation between the curvilinear system $(\bar{\xi}, \bar{\zeta})$ and the Cartesian co-ordinate system (x, z) is shown in Figure 1. Two-dimensional unsteady boundary-layer equations for this co-ordinate system can be written as :

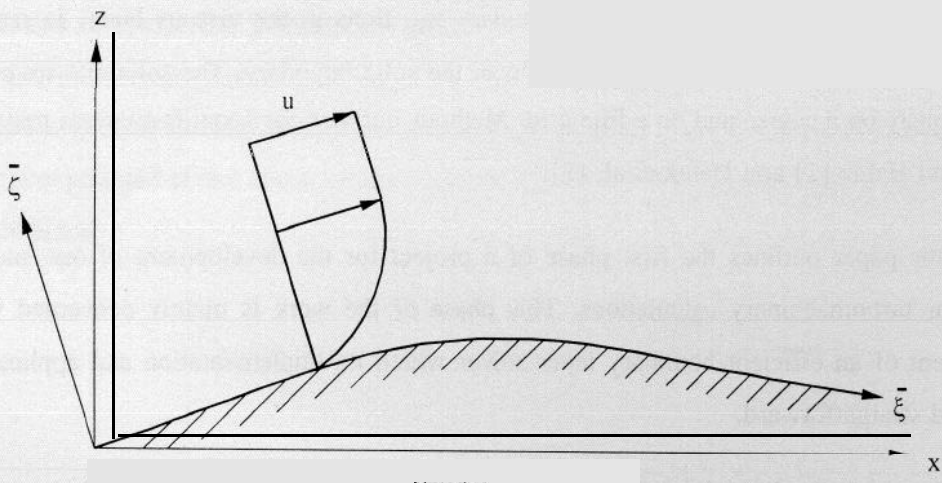


Figure 1 Notation for the calculation

Continuity equation

$$\frac{\partial \rho}{\partial t} + \frac{1}{h} \left[\frac{\partial(\rho u)}{\partial \bar{\xi}} + \frac{\partial(h_1 \rho w)}{\partial \bar{\zeta}} \right] = 0 \quad (1)$$

$\bar{\xi}$ momentum equation

$$\rho \left(\frac{\partial u}{\partial t} + \frac{u}{h} \frac{\partial u}{\partial \bar{\xi}} + v \frac{\partial u}{\partial \bar{\zeta}} \right) = - \frac{1}{h} \frac{\partial p}{\partial \bar{\xi}} + \frac{\partial}{\partial \bar{\zeta}} \left(\mu \frac{\partial u}{\partial \bar{\zeta}} \right) \quad (2)$$

Energy equation

$$\rho \frac{\partial H}{\partial t} + \frac{\rho u}{h_1} \frac{\partial H}{\partial \xi} + \rho w \frac{\partial H}{\partial \zeta} = \frac{\partial}{\partial \zeta} \left[\frac{\mu}{Pr} \frac{\partial H}{\partial \zeta} - \rho c_p \overline{w'T'} \right] + \frac{\partial}{\partial \zeta} \left[\left(\mu + \frac{\mu}{Pr} \right) u \frac{\partial u}{\partial \zeta} \right] + \frac{\partial}{\partial \zeta} \left[-\rho u u' w' \right] \quad (3)$$

The boundary conditions for the governing equations are given below.

at wall $\zeta = 0$: no-slip condition, $u = w = 0$

either a specific temperature, $T = T_b$

or heat-transfer condition, $\frac{\partial T}{\partial \zeta} = q$ or $H = H_b$ (4)

at the edge of boundary layer $\zeta \rightarrow \infty$

a specified free-stream conditions,

$u = u_e, T = T_e$ or $H = H_e$ (5)

where h_1 is the metric stretching factor

$$h_1 = \sqrt{\left(\frac{\partial X_b}{\partial \xi} \right)^2 + \left(\frac{\partial Z_b}{\partial \xi} \right)^2} \quad (6)$$

For more detail of these transformations see Yamazaki [8]. The subscript b means the value at the body surface $\zeta = 0$ and subscript e means the value at the edge of boundary-layer.

TURBULENCE MODEL

The turbulent shear stress $-\rho u' w'$ and the turbulent heat flux $-\rho c_p \overline{w'T'}$ may be evaluated in terms of the turbulent viscosity (μ_t) and the turbulent Prandtl number (Pr_t) [3].

$$\tau_{\parallel} = -\rho u' w' = \mu_t \frac{\partial u}{\partial \zeta} \quad (7)$$

$$\rho c_p \overline{w'T'} = \frac{\mu_t}{Pr_t} \frac{\partial T}{\partial \zeta} \quad (8)$$

Experimental results indicate that the turbulent Prandtl number based on the turbulent eddy viscosity and conductivity is a constant, usually taken as about 0.9. Therefore the turbulent modeling problem is reduced to the evaluation of the turbulent eddy viscosity. In this paper the eddy viscosity model suggested by Baldwin and Lomax [13] is used.

NUMERICAL METHOD

Since the boundary layer flows contain severe velocity gradients normal to the surface, an accurate solution of the boundary layer equations requires a very fine mesh near the wall. It is customary to use some forms of similarity transformation. These transformations however, are not entirely satisfactory for computing the entire range of laminar, transitional and turbulent boundary layers. One of the efficient ways of solving the boundary layer equations is to transform the equations before attempting to solve them. This technique may stretch such co-ordinate in order to account for boundary layer growth. For this propose a variable grid spacing is formed by using a geometric series such that the quotient of two consecutive terms is constant. Therefore, the distance to the k^{th} grid line is given by

$$\Delta \bar{\zeta}_k = \Delta \bar{\zeta}_1 \frac{(RY^{k-1} - 1)}{(RY - 1)} \quad (9)$$

where RY is grid growth factor and is a number greater than 1.

$\Delta \bar{\zeta}_1$ is the distance from the solid wall to the first grid line.

For turbulent flow calculations, the value of $\Delta \bar{\zeta}_1$ is chosen so that the first grid point away from the wall is placed approximately $\Delta \bar{\zeta}_1 \approx 1.5$ (defined as $\Delta \bar{\zeta}_1 \left(\frac{\rho_b \tau_b}{\mu_b} \right)^{1/4}$) in order to resolved the laminar sublayer.

The physical mesh is now non-uniformly spaced and we can relate this non-uniformly grid system $(\bar{\xi}, \bar{\zeta})$ to the uniformly grid system (ξ, ζ) (see Figure 2) through $\bar{\xi} = \xi$ and $\bar{\zeta} = \zeta$ [14]. Therefore the equations can be written as:

$$\frac{\partial p}{\partial t} + \frac{1}{h_1} \left[\frac{\partial(\rho u)}{\partial \xi} + \zeta_{\xi} \frac{\partial(\rho u)}{\partial \zeta} \right] + \zeta_{\zeta} \frac{\partial(\rho w)}{\partial \zeta} = 0 \quad (10)$$

$$\rho \frac{\partial u}{\partial t} + \frac{\rho u}{h_1} \frac{\partial u}{\partial \xi} + \frac{\rho u}{h_1} \zeta_{\xi} \frac{\partial u}{\partial \zeta} + \rho w \zeta_{\zeta} \frac{\partial u}{\partial \zeta} = -\frac{1}{h_1} \frac{\partial p}{\partial \xi} + \zeta_{\zeta} \frac{\partial}{\partial \zeta} \left(\mu \zeta_{\zeta} \frac{\partial u}{\partial \zeta} \right) \quad (11)$$

$$\rho \frac{\partial H}{\partial t} + \frac{\rho u}{h_1} \frac{\partial H}{\partial \xi} + \frac{\rho u}{h_1} \zeta_{\xi} \frac{\partial H}{\partial \zeta} + \rho w \zeta_{\zeta} \frac{\partial H}{\partial \zeta} = \zeta_{\zeta} \frac{\partial}{\partial \zeta} \left[\frac{\mu}{Pr} \zeta_{\zeta} \frac{\partial H}{\partial \zeta} + \mu \left(1 - \frac{1}{Pr} \right) u \zeta_{\zeta} \frac{\partial u}{\partial \zeta} \right] \quad (12)$$

In the above equations, the viscosity is the sum of molecular and eddy viscosity (i.e. $\mu = \mu + \mu_t$ and $\frac{\mu}{Pr} = \frac{\mu}{Pr} + \frac{\mu_t}{Pr_t}$). The subscripts $\bar{\xi}$ and $\bar{\zeta}$ in the equations mean differentiation with respect to $\bar{\xi}$ and $\bar{\zeta}$ respectively. The barred term is a non-uniformly spaced computational grid.

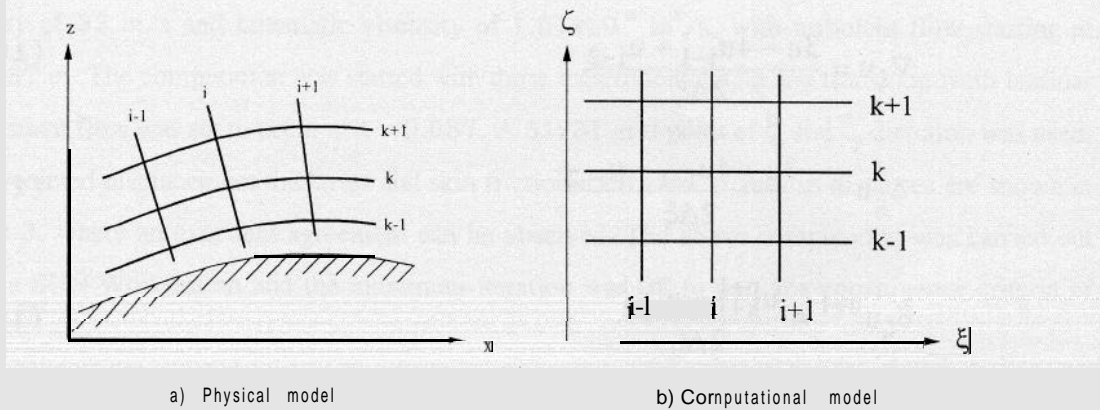


Figure 2 Curvilinear Body-fitted co-ordinate transformation

DISCRETISATION

The momentum and energy equations are solved by using a time-like algorithm. In this method the derivatives along the surface (i.e. $\frac{\partial}{\partial \xi}$) are represented by an explicit second-order accurate upwind difference, while the derivatives normal to the surface (i.e. $\frac{\partial}{\partial \zeta}$) are discretised by an implicit second-order accurate central difference. The time derivative in the governing equation is approximated for an expansion level $n+1$ with forward differencing. The resulting equations are non-linear due to presence of terms such as ρu in the momentum equation. To linearise the equations, it is possible to use Newton linearisation or simply to use a lagging technique in which all the coefficients are evaluated using the previous iteration results (i.e. the value at time level n are used to solve the equation for time level $n+1$). The latter iterative approach is implement in this case. Using normal finite difference operators the discretised form of momentum and energy equation can be written as:

$$\rho \Delta_t u + \frac{\rho}{h_1} \left[\frac{(u+|u|)}{2} \nabla_\xi u \right] + \frac{\rho}{h_1} \left[\frac{(u-|u|)}{2} \Delta_\xi u \right] + \frac{\rho u}{h_1} \zeta_\xi \delta_\zeta u^{n+1} + \rho w \zeta_\zeta \delta_\zeta u^{n+1} = -\frac{1}{h_1} \nabla_\zeta p + \zeta_\zeta \delta_\zeta \left(\mu \zeta_\zeta \delta_\zeta u^{n+1} \right) \quad (13)$$

$$\rho \Delta_t H + \frac{\rho}{h_1} \left[\frac{(u+|u|)}{2} \nabla_\xi H \right] + \frac{\rho}{h_1} \left[\frac{(u-|u|)}{2} \Delta_\xi H \right] + \frac{\rho u}{h_1} \zeta_\xi \delta_\zeta H^{n+1} + \rho w \zeta_\zeta \delta_\zeta H^{n+1} = \zeta_\zeta \delta_\zeta \left[\frac{\mu}{Pr} \zeta_\zeta \delta_\zeta H^{n+1} + \mu \left(1 - \frac{1}{Pr} \right) u \zeta_\zeta - \delta_\zeta u^{n+1} \right] \quad (14)$$

The operator notations used here are:

$$\Delta_t u = \frac{u^{n+1} - u}{\Delta t} \quad (15a)$$

$$\nabla_{\xi} u = \frac{3u - 4u_{i-1} + u_{i-2}}{2\Delta\xi} \quad (15b)$$

$$\Delta_{\xi} u = \frac{-3u + 4u_{i+1} - u_{i+2}}{2\Delta\xi} \quad (15c)$$

$$\delta_{\zeta} u^{n+1} = \frac{u_{k+1}^{n+1} - u_{k-1}^{n+1}}{2\Delta\zeta} \quad (15d)$$

The algebraic set of equations represented by the above equations can be solved for the unknown velocity u and total enthalpy H quite efficiently by inverting a tridiagonal matrix. Once u and H are found density and dynamic viscosity is updated. Then the continuity equation is solved to compute w . The continuity equation is discretised in the following way:

$$\Delta_i \rho + \frac{1}{h_i} \nabla_{\xi} (\rho u)^{n+1} + \frac{1}{h_i} \zeta_{\xi} \delta_{\zeta} (\rho u)_{k+1/2}^{n+1} + \zeta_{\zeta} \delta_{\zeta} (\rho w)_{k+1/2}^{n+1} = 0 \quad (16)$$

COMPUTATIONAL PROCEDURE

In the present computation, a time-marching scheme is employed however it is applied for steady flow. Using the discretization described in the previous section and the definition of eddy viscosity, the conservative equations are in a form of a tridiagonal system of equations that can be solved in an uncoupled manner. The momentum equation is solved for u^{n+1} , the energy equation for H^{n+1} , equation of state for T^{n+1} and ρ^{n+1} , viscosity law for μ^{n+1} and continuity equation for w^{n+1} . Finally, Baldwin-Lomax model is used to find μ_1^{n+1} . This sequence represents one cycle of an iteration procedure. The next time step is to update these values and the calculation is repeated until the difference between the two successive values of u be less than a specified tolerance (usually $\approx 1 \times 10^{-4}$). If the convergence criterion is not satisfied, all the parameters are updated and the process is repeated.

RESULTS

In order to validate the method, the computer program was constructed and applied to the test cases ranging from a flat plate to a more complex geometry. The calculations were started from the leading edge to the trailing edge using only the free-stream values of all parameters and the specified geometry.

The turbulent boundary layer that develops on a flat plate (a 5m long waxed plywood) is reported in case 1400 of [15]. It is incompressible flow. The measurement was taken with air

velocity of 33 m/s and kinematic viscosity of $1.51 \times 10^{-5} \text{ m}^2/\text{s}$ with turbulent flow starting at $x > 0.087$ m. The computation was started with those experimental data and transition from laminar to turbulent flow was set to occur at $x = 0.087$. A 51×31 grid point of ξ and η direction was used. The predicted displacement thickness and skin friction coefficient at various distances are shown in Figure 3, where an excellent agreement can be observed. The above computation was carried out using a SUN Workstation and the maximum iteration was 37 to pass the convergence criteria of 1×10^{-4} .

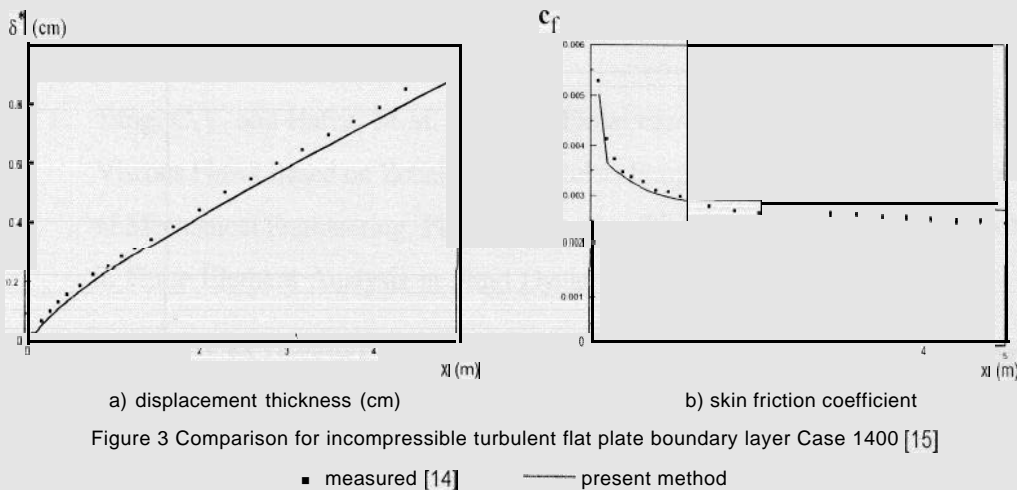


Figure 3 Comparison for incompressible turbulent flat plate boundary layer Case 1400 [15]

To extend the method for complex geometry, boundary layer on a waisted body of revolution was employed. A set of these experimental results for compressible turbulent boundary layer was presented in [16]. The geometry and computational grid is shown in Figure 4. The shape was specified in term of the distance from nose over the body length (x/L) and the body radius over the body length (z/L) where L is 1.52 m. The experimental skin-friction values were obtained by the razor blade technique. Only the measured free-stream Mach number distribution along the distance from nose was available. The computational grid used for the calculation of the flow consisted of a 51×31 mesh. To obtain the intermediate values of free-stream velocity from the measured data a cubic spline interpolation was used. It was given that the flow over this body of revolution accelerates up to about $x=0.3$ and is then followed by a decelerating flow up to $x=0.7$. Comparison of the predicted and measured skin friction coefficient at $M_\infty=0.6$ and 2.0 are presented in Figures 5 and 6 respectively. In each case the calculation results for both cases correlate well with the measurements for $x < 0.7$. The less accurate prediction for $x > 0.7$ may be attributed to the accumulation of the error from the calculation since no experimental data for the free-stream values were available for $x < 0.05$. It should also be noted that the effect of transverse-curvature is high where the radius of the body is quite small, for example when $x/L = 0.6-0.8$. The convergence criteria in this case is 1×10^{-5} and it was needed about 24 iterations (average) to satisfy the convergence criteria. The more iterations are needed where the flow was decelerated due to the existing adverse pressure gradient there.

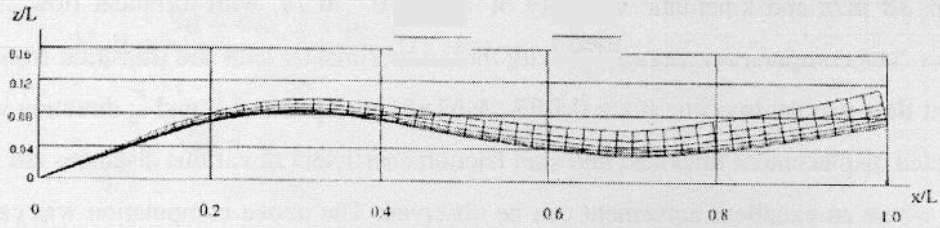


Figure 4 Geometry and computational grid for the waisted body of revolution

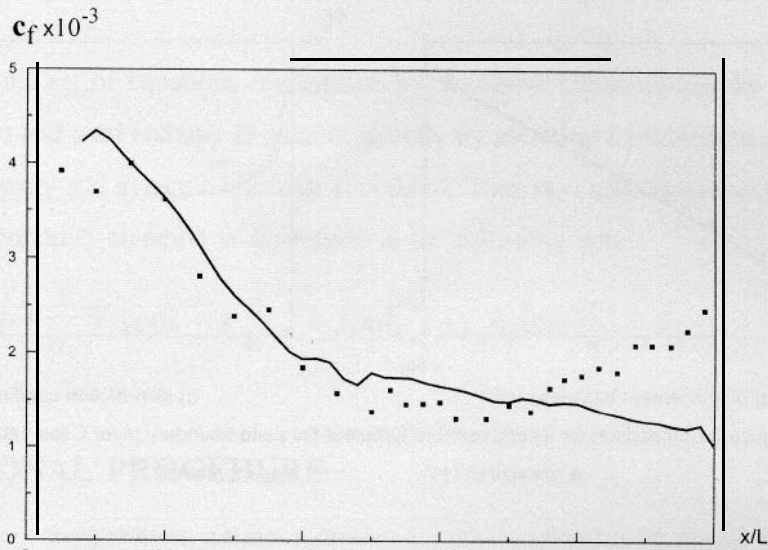


Figure 5 Comparison of skin friction coefficient for waisted body of revolution $M_\infty = 0.6$
 ■ measured [16] — present method

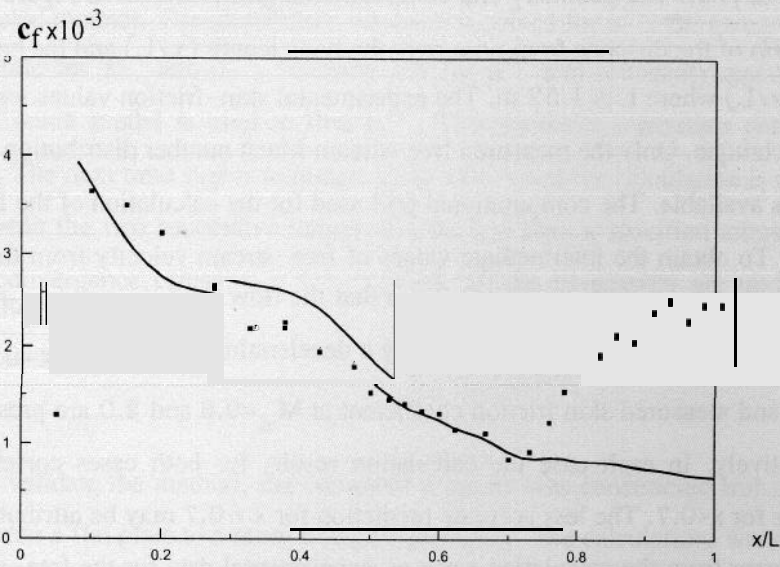


Figure 6 Comparison of skin friction coefficient for waisted body of revolution $M_\infty = 2.0$
 ■ measured [16] — present method

CONCLUSION

The equations and procedures described in this paper are general and can be applied to flow over complex geometry. The basic methodology of the present method is to time-march the unsteady boundary-layer equations of flow to steady state. However, its application restricts to the 2D flow on a stationary model. The method developed in this study has a potential to take into account of 3D flow and rotation. This is a next step for future research.

REFERENCES

1. Tang, C.Y. and Hafez, M.M., 1993, "Finite Element/Finite Volume Simulations of Viscous Flows Based on Zonal Navier-Stokes Formulations: Part I," American Society of Mechanical Engineering, Fluid Engineering Division (Publication) FED: Advances in Finite Element Analysis in Fluid Dynamics Vol. 17 1, pp. 5 3 - 6 5
2. Hafez, M.M., Habashi, W.G. and Przybytkowski, S.M., 1991, "Transonic Viscous-Inviscid Interaction by a Finite Element Method," *International Journal for Numerical Methods in Fluids*, vol.13, pp.309-319,
3. Anderson, D.A., Tannehill, J.C., and Pletcher, R.H., 1984, *Computational Fluid Mechanics and Heat Transfer*, Hemisphere Publishing Corporation.
4. Cebeci, T. and Smith, A.M., 1974, *Analysis of Turbulent Boundary Layers*, Academic Press, New York.
5. White, F.M., 1991, *Viscous Fluid Flow*, McGraw-Hill International, 2nd edition.
6. Fletcher, C.A.J., 1991, "Computational Techniques for Fluid Dynamics," Volume I-II, Second Edition, Springer-Verlag.
7. Lakshminarayana, B., 19 9 1, "An Assessment of Computational Fluid Dynamic Techniques in the Analysis and Design of Turbomachinery-The 1990 Freeman Scholar Lecture", *Journal of Fluid Engineering*, Vol. 113, September 19 9 1, pp. 3 1'5 - 35 2.
8. Yamazaki, R., 1981, "On the Theory of Marine Propellers in Non-uniform Flow," *Memoirs of the Faculty of Engineering, Kyushu University*, Vol. 41, No. 3, September 1981.
9. Groves, N.C. and Change, M.S., 1984, "A Differential Prediction Method for 3-D Laminals and Turbulent Boundary Layers of Rotating Propeller Blades," *The 15th Symposium on Naval Hydro-dynamics*, 6 Sep 1984

10. Oshima, A., 1994, "Analysis of Three-dimensional Boundary-layer on Propeller Blade," *Propellers/shafting'94* symposium, September 20-21, 1994.
11. Zangeneh, M. and Asvapoositkul, W., 1993, "A Method for the Calculation of 2D Compressible Laminar and Turbulent Boundary Layers," *Proc. Intl. Congress on Computational Methods in Engineering*, Shiraz Iran, May 2-6, 1993, Yanghoubi H.A. Shiraz University Press.
12. Steger, J.L. and Van Dalsem, W.R., 1985, "Development in the Simulation of Separated Flows Using Finite Difference Methods," *Proceeding of the Third Symposium on Numerical and Physical Aspects of Aerodynamic Flows*, California State University, Long Beach, Cal., January, 1985.
13. Baldwin, B.S. and Lomax, H., 1987, "Thin Layer Approximation and Algebraic Model for Separated Turbulent Flow," *AIAA paper 78-257*
14. Warsi, Z.U.A., 1992, *Fluid Dynamics Theoretical and Computational Approaches*, CRC Press.
15. Coles, D.E. and Hirst, E.A., 1968, "Computation of Turbulent Boundary Layers," *AFOSR-IFP Stanford Conference, Proc. 1968 Conf.*, Vol. 2, Stanford University.
16. Winter, K.G., Smith, K.G. and Rotta, J.C., 1965, "Turbulent Boundary Layer Studies on a Waisted Body of Revolution in Subsonic and Supersonic Flow," *AGARDograph 9'7*, Part II, May 1965

NOMENCLATURE

c_f	skin-friction coefficient $\frac{\tau_w}{\frac{1}{2} \rho_e u_e^2}$
c_p	specific heat at constant pressure
h_{ij}	metric coefficients
H	total enthalpy
i, j	index of the grid point system
k	thermal conductivity
M	Mach number
n	iteration level, time step, index of time
P	static pressure
Pr	Prandtl number $\left(\frac{c_p \mu}{k} \right)$
T	temperature

t

u, w

δ^*

$\Delta n, \Delta \xi, \Delta \zeta$

$\Delta x, \Delta z$

μ

v

ρ

τ